



Study on mechanism of starch phase transition in wheat with different moisture content

Lei SU¹, Fengjuan XIANG¹, Renbing QIN¹, Zhanxiang FANG¹, Jie ZENG¹, Guanglei LI^{1*} 

Abstract

Using Bainong 365 wheat starch as raw material, starch samples were preheated in a RVA to simulate DSC heating profiles. The thermodynamic properties, long-range orderliness, short-range orderliness, and structure of wheat starch were determined by DSC, XRD, FTIR, LF-NMR and SEM to explore the phase transformation mechanism of Bainong 365 wheat starch at different water contents. The results show that at different moisture contents, when the endothermic transition temperature of starch samples determined by DSC was reached or exceeded, the enthalpy of starch was 0, all free water was converted into unbound water and bound water, and the surface structure of starch was severely damaged. At this time, starch was completely gelatinized, but the short-range and long-range ordered structures of starch determined by FTIR and XRD still existed and gradually decreased with increasing temperature. Therefore, it was concluded that the temperature range of the starch endothermic transition does not represent the temperature range of complete gelation of starch, and the structure destroyed by complete gelation of starch may not be simple short-range and long-range ordered molecular structures.

Keywords: wheat starch; phase transition mechanism; thermodynamic characteristics; long-range order; short-range order; water transport characteristic.

Practical Application: Mechanism of starch phase transformation in wheat.

1 Introduction

Wheat starch is a natural macromolecular polysaccharide compound, and it is mainly divided into the two categories of A-type starch and B-type starch. It is composed of amylose and amylopectin. Amylose is linearly linked by α -1,4 glycosidic bonds, while amylopectin has a highly branched structure linked by α -1,4 and α -1,6 glycosidic bonds (Chen et al., 2011). Wheat starch chains aggregated to form spiral structures, spirals aggregated to form microcrystalline structures, and then these microcrystalline structures form alternating amorphous and crystalline lamellae (Gilbert et al., 2013).

Starch phase transformation refers to the infiltration of amylose into starch molecules after starch gelatinization and the formation of a three-dimensional network structure by intertwining with each other in the form of a double helix. The fully gelatinized starch particles are wrapped in this double helix. This process is called phase transformation, namely, the gelation process (Donovan, 1979). Starch gelation is a complex process rather than a simple particle transformation process from order to disorder (Chen et al., 2015). In recent years, the theme of wheat starch research in China and abroad has been increasingly in-depth, and a large number of research results have been produced. It has been previously reported that wheat starch maintains its original A-type crystal structure after annealing, annealing treatment improves the crystallinity, amylopectin short chain, viscosity and gelatinization temperature of starch, and the annealing reduces the in vitro digestibility of wheat starch (Su et al., 2020). The hydrothermal changes of starch were monitored by nuclear magnetic resonance (NMR) and

differential scanning calorimetry (DSC), and it was found that in the corresponding temperature range (55~70 °C), the change in the first phase transition enthalpy of the starch-water mixture was strongly correlated with the solid content loss measured by NMR (Kovrlja & Rondeau-Mouro, 2017).

Studies have shown that moisture content and heating temperature affect the variability of starch structure, thereby affecting the functional properties of starch (Colussi et al., 2020; Gercekaslan, 2021; Selma-Gracia et al., 2020). However, the specific mechanism of this influence is not clear. Therefore, it is necessary to conduct in-depth research on starch structure, moisture content and heating temperature to further reveal the intrinsic relationship among them. In this paper, Bainong 365 wheat starch was used as the raw material, and the samples were prepared by RVA simulation DSC. Differential scanning calorimetry (DSC), X-ray diffraction (XRD), Fourier transform infrared spectroscopy (FTIR), low-field nuclear magnetic resonance (LF-NMR) and scanning electron microscopy (SEM) were used to study the multiscal structures and water migration characteristics of the samples. The results obtained will help to better understand the mechanism of starch gelation and starch structure.

2 Materials and methods

2.1 Materials

Bainong 365 wheat gains were provided by the Henan Institute of Science and Technology (Xinxiang, China). All other

Received 11 Oct., 2021

Accepted 17 Nov., 2021

¹School of Food Science, Henan Institute of Science and Technology, Xinxiang, China

*Corresponding author: lg170_hist@163.com

chemical reagents utilized in this study were of analytical grade and were used without further purification.

2.2 Starch isolation

The wheat starch was isolated using the method described by Wang et al. (2015), with a slight modification.

First, 500 g of wheat seeds were soaked in 2000 mL ammonia solution (0.2 mol/L) for 12 h. Then, the supernatant was discarded, and the soaked wheat seeds were mixed with freshly prepared ammonia solution at a ratio of 1:3 (w/v) with a beating machine (BARBOSA Babosa Brand Store, China) (the beating machine was stopped for 2 minutes every 3 minutes to prevent, overheating). The obtained slurry was filtered with a 150 μm filter to obtain filtrate 1. The remaining filter residue on the filter screen was added to the ammonia solution, and the slurry was filtered again. The filtrate was mixed with filtrate 1, and filtrate 2 was obtained. Then, the filtrate 2 was centrifuged at 3600 r/m (low-speed centrifuge, L550, Hunan, China) for 15 min, the supernatant was discarded, and the upper yellow precipitate was scraped. The obtained white precipitate was resuspended in ammonia solution and centrifuged, and the yellow precipitate in the supernatant and the upper layer was discarded. This operation was repeated at least three times. The obtained precipitate was suspended in acetic acid solution (0.2 mol/L) and filtered through 75 μm filter cloth to obtain filtrate 3. Filtrate 3 was centrifuged at 3600 r/m for 15 min to obtain crude starch. The obtained crude starch was repeatedly washed and centrifuged with distilled water for more than three times (until the pH value of the supernatant was determined to be 7 with pH test paper). Finally, the obtained precipitate was mixed with anhydrous ethanol and filtered, and this process was repeated twice. The obtained starch was dried at room temperature and stored in a closed container at 4 $^{\circ}\text{C}$ for further use.

2.3 Basic components

The moisture, ash, protein and fat in this starch were determined using the AOCO method.

The amylose content was determined according to the procedure of Chrastil (1987), with a slight modification.

2.4 Thermodynamic properties

The thermal properties of Bainong 365 wheat starch were determined by differential scanning calorimeter (DSC, Q200, TA, USA). Samples (3.0 mg) were accurately weighed into a DSC crucible, and distilled water was added to obtain 33.3%, 50%, 60%, 75% and 80% starch-water mixtures. The starch and water were mixed uniformly, sealed, and placed at room temperature for 12 h before DSC measurement. During DSC, the samples were heated from 20 $^{\circ}\text{C}$ to 95 $^{\circ}\text{C}$ at a rate of 10 $^{\circ}\text{C}/\text{min}$. The temperature of the starch phase transition was obtained by the analysis software of the instrument, including the initial temperature T_o , the peak temperature T_p , the termination temperature T_c and the enthalpy ΔH .

2.5 Preparation of starch samples by RVA

The starch samples were prepared according to the procedure of Wang et al. (2016) with slight modification. The starch sample (3.0 g) was accurately weighed into RVA canisters, and distilled water was added to obtain 33.3%, 50%, 66.7%, 75% and 80% starch-water mixtures. The RVA barrel was sealed and marked with a plug, and then placed at room temperature for 4 h, and then the temperature of T_o-10 , T_o , T_p , T_c and T_c+10 wulated according to DSC. The prepared samples were heated to the temperature measured by DSC in a RVA, that is, the initial temperature of heating was 20 $^{\circ}\text{C}$, the heating rate was 10 $^{\circ}\text{C}/\text{min}$, and the end temperature of heating corresponded to the temperature by DSC. The samples were quickly placed into the refrigerator at -18 $^{\circ}\text{C}$ for 24 h and then freeze-dried by a vacuum freeze-drying machine (Aiphal-2LDplus, CHRIST, Germany) and ground into powders that passed through a 100 μm sieve. The control sample was prepared with 80% moisture content.

2.6 Scanning electron microscopy

The particle morphologies of the starch samples were measured by scanning electron microscope (SEM, Quanta 200, FEI, USA). A small amount of starch particles were uniformly adhered to the aluminum carrier with conductive adhesive cloth, and the carrier table was placed into the gold plating instrument. The sample was carbonized by ion sputtering coating for 90 s and then observed using scanning electron microscopy (Oliveira et al., 2021; Zhang et al., 2020).

2.7 X-ray diffraction

The samples were equilibrated over ultrapure water for 24 h, and then evaluated using an X-ray diffractometer (XRD, D8 Advance A25, Bruker, Germany) operating at 40 kV and 30 mA. The scanning range was from 4 $^{\circ}$ to 40 $^{\circ}$ (2 θ), the scanning rate was 2 $^{\circ}/\text{min}$, and the step size was 0.02 $^{\circ}$. The relative crystallinity was calculated by Jade 6.0 software (Wang et al., 2017).

2.8 Fourier transform infrared spectroscopy

The short-range order of the starch samples was determined by Fourier transform infrared spectroscopy (FTIR, TENSOR 27, Bruker, Germany). Samples (2 mg) were ground with KBr powder (150 mg) in an agate mortar and then pressed into round tablets (to prevent the grinding process from always occurring under the infrared lamp). The spectra were scanned in the range of 400~4000 cm^{-1} . Spectra were analyzed by OMNIC 8.3 software. The ratio of absorbances at 1047/1022 cm^{-1} was obtained to characterize the short-range molecular order of starch samples (Su et al., 2020).

2.9 Low field nuclear magnetic resonance

The samples obtained by simulated DSC heating were cooled for 15 min in a refrigerator at 4 $^{\circ}\text{C}$. After stirring evenly, the samples were poured into glass bottles with an inner diameter of 25 mm and height of 50 mm. Then the glass bottles were placed in NMR tubes, and the NMR tubes were placed in the center of the RF coil at the center of the low field nuclear magnetic

resonance (LF-NMR, NMI20-040V-I, Suzhou, China), and the CPMG sequence was applied, with three parallel determinations for each sample. The sequence parameters were as follows: magnet temperature, 32 °C; 90° pulse width, 6.25 us; 180° pulse width, 13.04 us; analog gain DRGI, 20; digital gain width, 3; sampling frequency SW, 200 kHz; repeat sampling points TD, 900008; and echo number NECH, 15000. Data inversion was performed after the tests, and the number of inversions was 100000 (Jiang et al., 2021).

2.10 Analytical calculations

All data are presented as the means \pm standard deviation (SD), and the statistical analysis was performed using Origin 18 data analysis software.

3 Results and analysis

3.1 Basic components of wheat starch

The amylose content of Bainong 365 wheat starch was 26.3% (Table 1), which was comparable to that usually reported for wheat starch (An et al., 2021; Zhao et al., 2020). The water content, ash content, protein content and fat content of Bainong 365 wheat starch were 9.71%, 0.13%, 0.18% and 0.17%, respectively.

3.2 Thermodynamic properties of native wheat starch

The DSC thermograms and corresponding thermal transition temperatures (T_o , T_p , T_c) and enthalpy change (ΔH) of the samples are shown in Figure 1 and Table 2, respectively. The T_o of the sample with 50% moisture content (MC) is slightly higher than that of the sample with 33.3% MC, which may be due to pyrodextrinization of starch at a low moisture content (Wang & Copeland, 2013). This may also be due to the fact that at lower moisture content, there is less free water in the starch system and thus the amount of energy available to destroy the crystal structure of starch is increased, resulting in a higher starting temperature (Schirmer et al., 2015). Overall with increasing water content, T_o and T_p gradually increased, while T_c changed little. The enthalpy (ΔH) of the samples reached a maximum of 9.79 J/g when the water content was 66.7%. As the water content

Table 1. Basic component content of wheat starch.

Water(%)	ash(%)	protein(%)	fat(%)	amylose(%)
9.71 \pm 0.2	0.13 \pm 0.07	0.18 \pm 0.12	0.17 \pm 0.10	26.30 \pm 0.70

Note: The values are mean \pm standard deviation.

Table 2. Thermal transition temperature of native wheat starch.

Water content(%)	T_o (°C)	T_p (°C)	T_c (°C)	ΔH (J/g)
33.3	61.26 \pm 0.6a	65.96 \pm 0.7b	85.30 \pm 0.0a	2.54 \pm 0.2c
50	59.19 \pm 0.1c	66.43 \pm 0.7ab	85.54 \pm 0.3a	7.40 \pm 0.0b
66.7	59.61 \pm 0.1bc	66.71 \pm 0.3ab	85.19 \pm .0.1a	9.79 \pm 0.7a
75	60.33 \pm 0.1abc	68.25 \pm 0.3ab	85.21 \pm 0.2a	9.60 \pm 0.5a
80	60.48 \pm 0.3ab	68.47 \pm 0.2a	85.01 \pm 0.1a	9.44 \pm 0.2a

Note: The values are mean + standard deviation, different letters in the same column indicated significant difference ($P < 0.05$).

increased further, the enthalpy did not significantly change, which was consistent with the research results of Wang et al. (2016).

3.3 Thermodynamic properties of prepared wheat starch samples

Figure 2 represents the gelation of Bainong 365 wheat starch samples RVA prepared at different temperatures. Only samples with 66.7% moisture content showed an enthalpy of 1.545 J/g when heated to T_c (Figure 2d). When heated to T_c+10 , no enthalpy was detected, indicating that starch gelled completely at high temperature. Under different moisture contents, the enthalpy of wheat starch samples decreased with increasing preparation temperature, indicating that the crystal structure of wheat starch was destroyed more completely with increasing temperature in the process of DSC heating, so the energy needed to destroy the crystal structure was reduced, thus, the enthalpy decreased (Hung et al., 2007). The ΔH of starch heated to t_o-10 was higher than that of T_o at 33.3%, 66.7% and 75% moisture contents, which may be due to the low temperature. The unstable crystals in starch gelatinized first, and some crystals may undergo the traditional melting transformation, resulting in additional DSC endotherms. Therefore, the ΔH of starch heated to T_o-10 was slightly higher than that of starch heated to t_o (Waigh et al., 2000). When heated to T_p , the ΔH of wheat starches with 75% and 80% MC were 6.832 J/g and 6.969 J/g, respectively. However, as the temperature increased to T_c and T_c+10 , the ΔH dropped

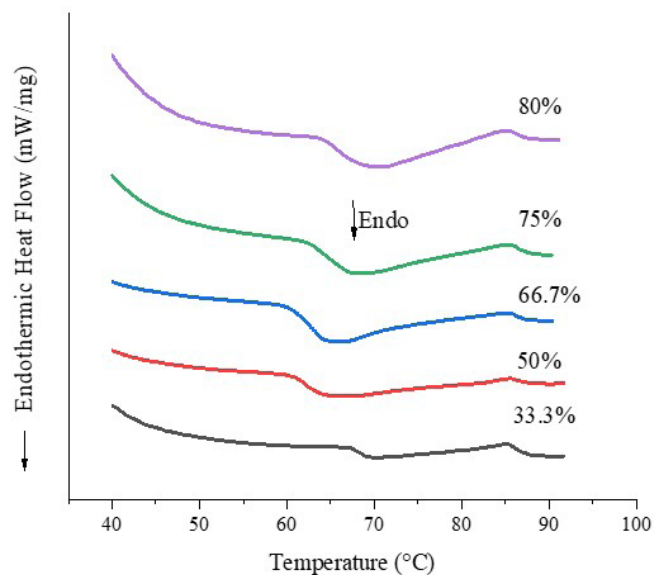


Figure 1. DSC curves of native wheat starch.

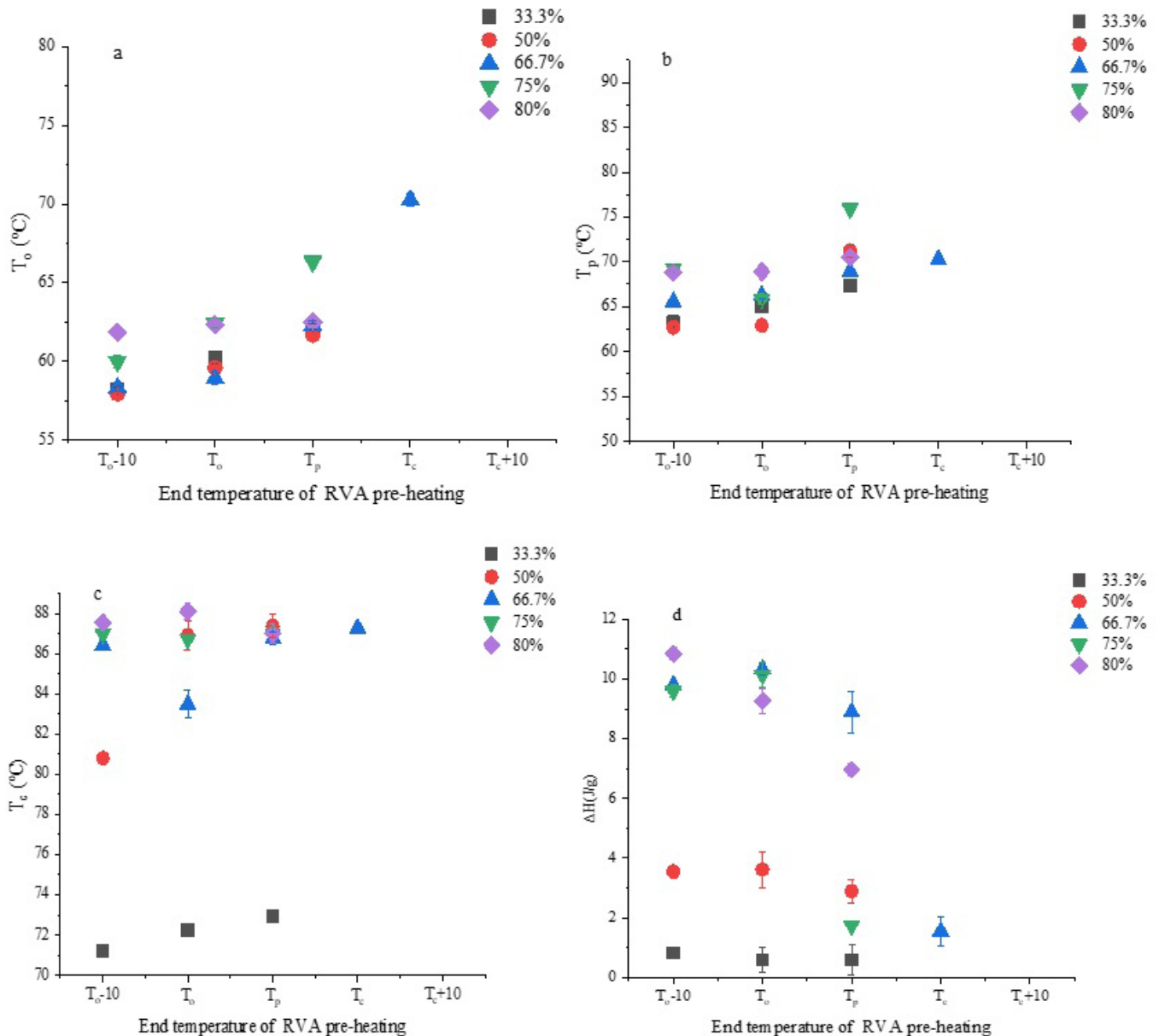


Figure 2. Thermal transition parameters of starch samples after pre-heating to different temperatures in RVA canisters (a: T_o of starch samples; b: T_p of starch samples; c: T_c of starch samples; d: ΔH of starch samples).

to 0, indicating that when the moisture content was high, with increasing temperature, the gelation rate of starch samples was fast, and the gelation of starch was more complete (Ratnayake & Jackson, 2007; Vermeylen et al., 2005).

3.4 Granule morphology of wheat starch samples

Figure 3 and 4 show the SEM images of wheat starch control samples and prepared samples. Figure 3 shows that the wheat starch control sample was disc-shaped, and some starch granules had pits on the surface, which was consistent with previous research results (Chen et al., 2011; Zhang et al., 2013). From Figure 4, it can be found that with increasing moisture content, when the sample preparation temperature was T_o-10 , the starch

granules swelled and the number of pits on the starch surface increased. At the sample preparation temperature of T_p , except for the sample with 33.3% moisture content, the adhesion and apparent morphology of other starch granules were destroyed. At 66.7% moisture content, the morphology of starch was damaged most seriously, and there were essentially no complete starch granules.

3.5 Long-range order of wheat starch samples

Figure 5a gives the XRD pattern of the Bainong 365 wheat starch control sample, and the relative crystallinity is 18.74%. The diffraction angle (2θ) of starch has obvious diffraction peaks at 15° , 17° , 18° and 23° , including that it contains typical A-type

crystals (Ee et al., 2020; Wang et al., 2017). The weak diffraction peaks at 20° were attributed to complexes between amylose and lipids (Chen et al., 2017; Sun et al., 2021).

It can be seen from Figure 5 that the samples prepared by heating wheat starch to T_o-10 , T_o , and T_p at different moisture contents had obvious diffraction peaks at 15°, 17°, 18° and 23°, that is, the prepared wheat starch samples contained A-type crystals, and the relative crystallinity was 4.35~13.6%; When the sample preparation temperature was T_c and T_c+10 at 75% MC, the intensity of the peaks decreased obviously, and the characteristic diffraction peaks even disappeared completely. The minimum relative crystallinity was 3.31%, which indicates that the crystal structure of the sample is damaged more seriously with increasing temperature (Xu et al., 2020). However, it can

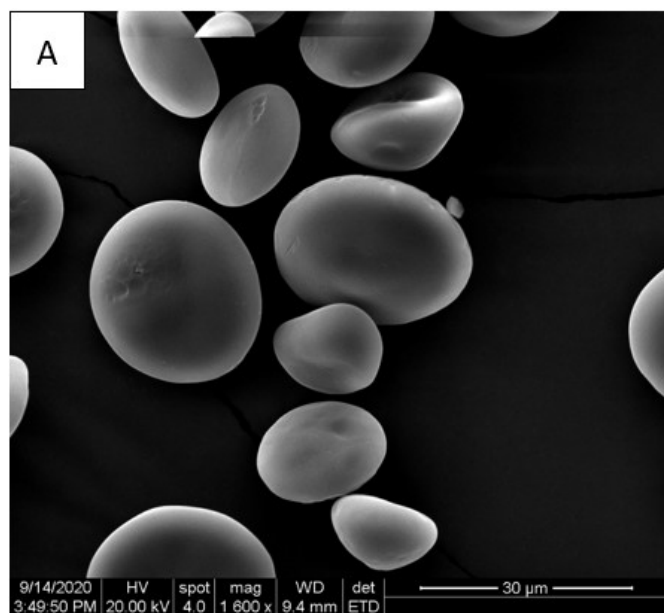


Figure 3. SEM images of the control samples. Magnification, 1600X.

Table 3. Relative crystallinity of wheat starch samples prepared.

水分含量(%)	T_o-10	T_o	T_p	T_c	T_c+10
33.3	13.60 ± 0.05a	13.53 ± 0.10a	10.94 ± 0.10a	9.80 ± 0.00a	6.11 ± 0.02a
50	12.21 ± 0.13b	12.80 ± 0.01b	9.23 ± 0.06b	4.67 ± 0.05b	3.32 ± 0.10b
66.7	11.03 ± 0.08c	10.95 ± 0.06c	8.60 ± 0.03c	4.72 ± 0.04c	3.50 ± 0.06c
75	10.50 ± 0.01d	10.23 ± 0.04d	4.35 ± 0.04d	3.50 ± 0.07c	3.31 ± 0.04d
80	9.98 ± 0.06d	9.70 ± 0.04d	6.74 ± 0.01e	6.06 ± 0.01d	3.77 ± 0.02e

Note: The values are mean + standard deviation, different letters in the same column indicated significant difference ($P < 0.05$).

Table 4. The ratios of absorbances at 1047/1022 cm^{-1} of starch samples.

Water content(%)	1047/1022 cm^{-1}				
	T_o-10	T_o	T_p	T_c	T_c+10
33.3	0.8615 ± 0.004 ^a	0.8596 ± 0.003 ^a	0.8517 ± 0.010 ^b	0.8498 ± 0.007 ^b	0.8419 ± 0.000 ^c
50	0.8592 ± 0.002 ^a	0.8529 ± 0.004 ^b	0.8517 ± 0.012 ^c	0.8340 ± 0.005 ^d	0.7983 ± 0.017 ^e
66.7	0.8641 ± 0.005 ^a	0.8577 ± 0.007 ^b	0.8516 ± 0.010 ^c	0.8427 ± 0.00 ^d	0.8380 ± 0.009 ^e
75	0.8639 ± 0.000 ^a	0.8576 ± 0.003 ^b	0.8564 ± 0.003 ^c	0.8478 ± 0.000 ^d	0.8418 ± 0.002 ^e
80	0.8726 ± 0.015 ^a	0.8660 ± 0.001 ^b	0.8593 ± 0.003 ^c	0.8429 ± 0.001 ^d	0.8329 ± 0.007 ^e

Note: The values are mean ± standard deviation, different letters in the same line indicated significant difference ($P < 0.05$).

be found from Table 3 that when the moisture content was 80%, with increasing heating temperature, the relative crystallinity decreased more slowly than that of starch with 75% moisture content. However, when the preparation temperature was T_c+10 , the crystallinity was higher than that of the 75% MC sample, which may be because the influence of high moisture content heating on the starch system was reduced by increased moisture. Under the same heating temperature with different moisture contents, the higher the moisture content is, the smaller the relative crystallinity is, indicating that the influence of moisture on the crystallinity of starch is particularly important.

3.6 Short-range order of wheat starch samples

The short-range order of starch was determined by Fourier transform infrared spectroscopy. The absorption peaks at 1047 cm^{-1} and 1022 cm^{-1} represented the characteristic peaks of the crystalline region and noncrystalline region of starch, respectively. $R_{1047/1022}$ represents the crystal short-range order structure of starch. The larger the ratio, the higher the short-range order of the starch molecule, and the more prevalent double helix structure (Van Soest et al., 1995).

The infrared spectra of different wheat starch preparation samples are shown in Figure 6, and the ratio of $R_{1047/1022}$ is shown in Table 4. The infrared spectra of wheat starch samples prepared with different water contents were similar. With increasing heating temperature, the ratio of $R_{1047/1022}$ gradually decreased, and the relative order gradually decreased, indicating that the higher the temperature was, the more the ordered structure of starch was destroyed. These results are consistent with the results obtained by DSC and XRD.

3.7 Water migration characteristics of wheat starch RVA prepared samples

Low-field nuclear magnetic resonance (LF-NMR) technology is often used in the field of food science due to its rapid and

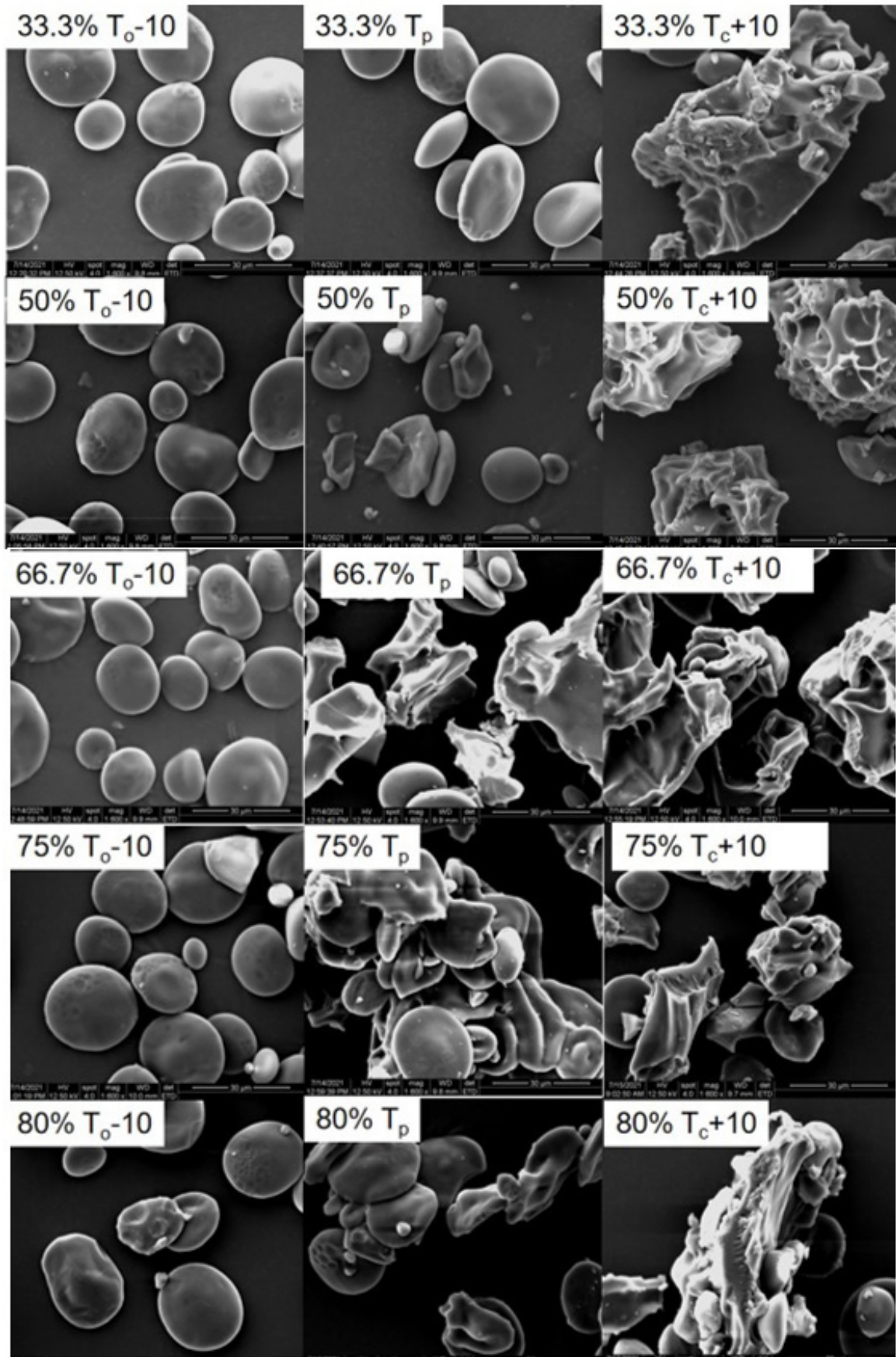


Figure 4. SEM images of wheat starch samples after preheating to different temperatures. Magnification, 1600X.

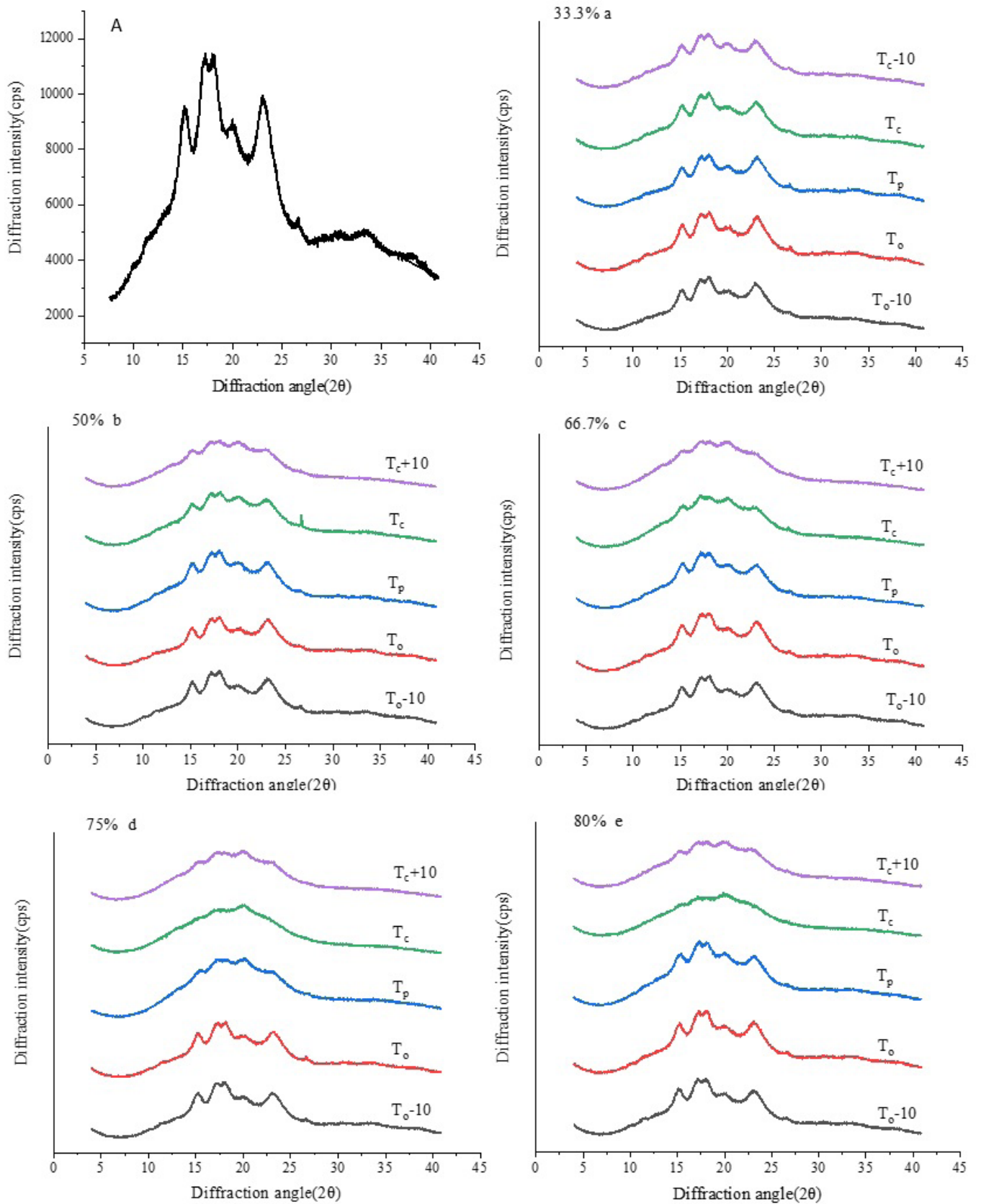


Figure 5. The XRD patterns of control samples(A) and starch samples(a~e).

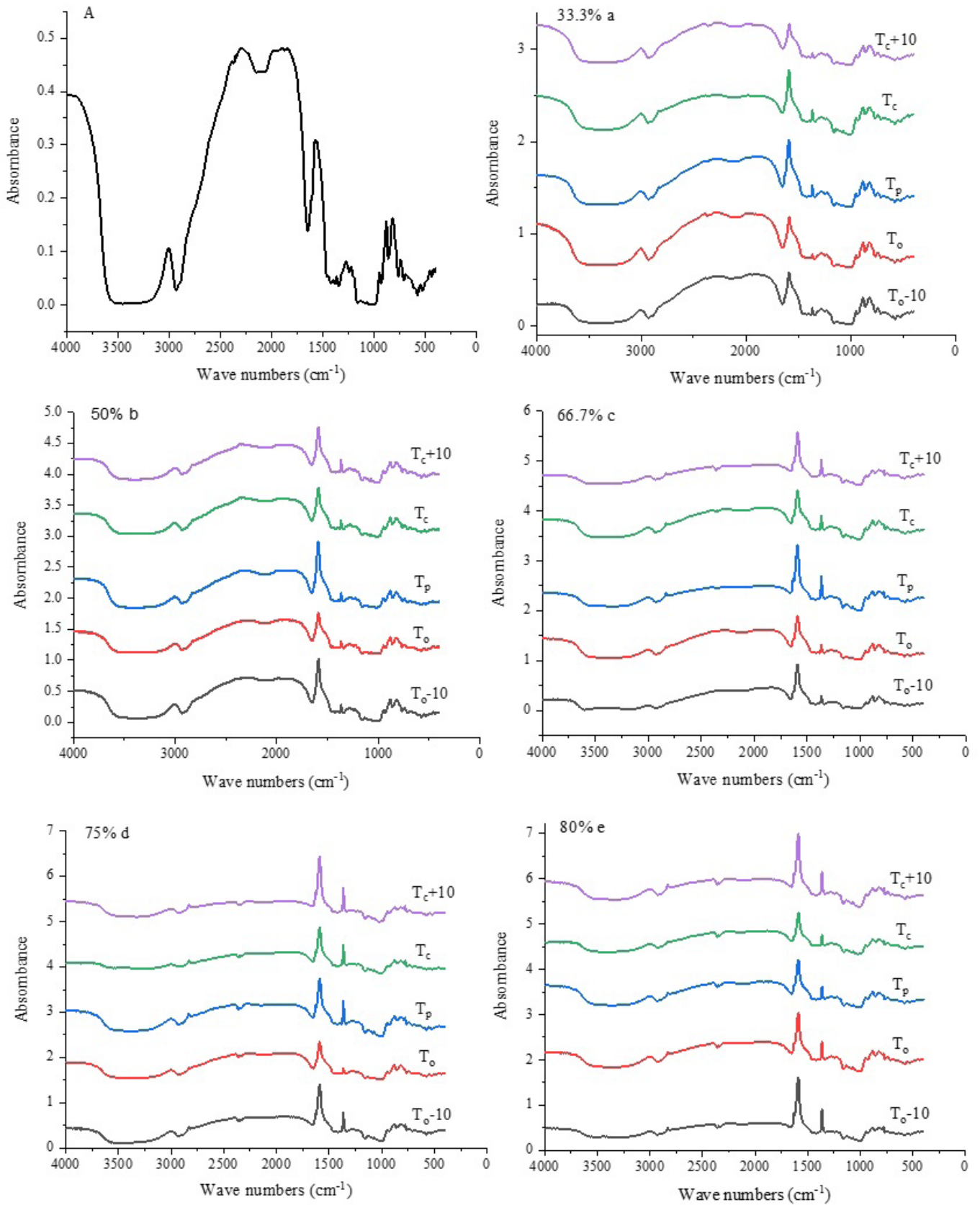


Figure 6. The FTIR spectre of control samples(A) and starch samples(a ~ e).

nondestructive detection characteristics. LF-NMR mainly reflects the state distribution and molecular binding of the sample by measuring the relaxation time (Hansen et al., 2009; Yao & Ding, 2002). When starch is heated to form a gel at a certain moisture content, there are many states of water inside it. Therefore, the spin-spin relaxation time (also known as transverse relaxation time and relaxation time, T_2) is very accurate for monitoring of the state distribution of water in a starch gel system. T_2 depends on the microenvironment of protons and is closely related to the binding force and degree of freedom of protons (Li et al., 2017). Relaxation time T_2 can distinguish bound water (T_{21}), uneasy flowing water (T_{22} and T_{23}) and free water (T_{24}). The corresponding peak areas of relaxation time are A_{21} , A_{22} , A_{23} and A_{24} . T_2 is positively correlated with the mobility of water molecules (Fan et al., 2013).

Table 5 and Figure 7 show the changes in the total moisture T_2 of wheat starch gels with different moisture contents. Under the same moisture content, with increasing heating temperature, the relaxation time of starch samples on the whole showed a gradually decreasing trend, even disappearing completely, and

the free water peak area also gradually decreased or reached 0, indicating its transformation into bound water and nonflowable water (Ozel et al., 2017; Zhang et al., 2019). At T_o-10 temperature and 33.3% MC, the peak time of T_{21} increased, which may be because the low moisture content at that heating temperature did not fully combine with the starch. At T_c+10 (water content 66.7%), T_p , T_c , T_c+10 (water content 75% and 80%) temperatures, the T_{24} peak disappears, that is, there is no free water. It may be that with the increase in temperature, higher water volume makes the interaction between starch and water more fully occur, and the molecules are rapidly tightly cross-linked and recombined, resulting in the conversion of free water into low fluidity bound water and nonflowable water, indicating that the gelation of starch is more complete and the water holding capacity is enhanced (Shang et al., 2021; Zhang et al., 2020).

Table 6 shows the changes in the total moisture peak area of wheat starch gels with different moisture contents. The relaxation time corresponds to water in different states, relative moisture content and peak area. It can be seen from the table that with the increase in temperature at 33.3% and 50% water content, the

Table 5. Changes in the total moisture T_2 of wheat starch gels with different moisture content.

	T_2 (ms)			
	T_{21}	T_{22}	T_{23}	T_{24}
33.3%				
T_o-10	0.38 ± 0.1a	7.01 ± 1.2a	-	705.48 ± 3.6d
T_o	0.04 ± 0.0b	6.14 ± 1.6b	-	613.59 ± 2.3c
T_p	0.03 ± 0.0b	5.34 ± 2.0c	-	533.67 ± 1.4a
T_c	0.03 ± 0.0b	-	28.48 ± 1.7a	533.67 ± 1.6a
T_c+10	0.03 ± 0.0b	-	24.77 ± 1.3b	464.16 ± 2.8b
50%				
T_o-10	0.03 ± 0.0a	9.33 ± 2.0a	200.92 ± 1.7a	1417.47 ± 0.0a
T_o	0.03 ± 0.0a	6.14 ± 1.7b	151.99 ± 0.9b	1417.47 ± 0.0a
T_p	0.03 ± 0.0a	-	132.19 ± 1.4c	613.59 ± 1.7b
T_c	0.03 ± 0.0a	-	120.45 ± 1.7d	464.16 ± 2.1c
T_c+10	0.03 ± 0.0a	-	107.36 ± 2.0e	305.39 ± 3.0d
66.7%				
T_o-10	0.03 ± 0.0a	24.77 ± 1.1b	-	705.48 ± 2.5a
T_o	0.05 ± 0.0b	18.74 ± 2.4c	-	613.59 ± 3.2b
T_p	0.03 ± 0.0a	12.33 ± 2.1d	-	533.67 ± 1.2c
T_c	0.03 ± 0.0a	14.18 ± 0.0a	-	300.45 ± 1.7d
T_c+10	0.03 ± 0.0a	14.18 ± 0.0a	-	-
75%				
T_o-10	0.03 ± 0.0a	4.64 ± 1.3b	37.65 ± 2.5a	811.13 ± 0.0a
T_o	0.03 ± 0.0a	7.01 ± 2.1c	32.75 ± 1.6b	811.13 ± 0.0a
T_p	0.03 ± 0.0a	1.32 ± 0.4a	21.54 ± 1.8c	-
T_c	0.03 ± 0.0a	1.75 ± 0.3a	16.30 ± 2.3d	-
T_c+10	0.03 ± 0.0a	2.01 ± 0.2d	12.33 ± 2.4e	-
80%				
T_o-10	0.33 ± 0.0b	6.14 ± 1.4b	75.65 ± 1.0c	1232.85 ± 0.0a
T_o	0.03 ± 0.0a	-	37.65 ± 2.3b	1072.27 ± 0.0b
T_p	0.03 ± 0.0a	1.32 ± 0.2a	16.30 ± 0.0a	--
T_c	0.03 ± 0.0a	1.32 ± 0.3a	16.30 ± 0.0a	-
T_c+10	0.03 ± 0.0a	1.75 ± 0.2c	37.65 ± 1.2b	-

Note: The values are mean ± standard deviation, different letters in the same column indicated significant difference ($P < 0.05$).

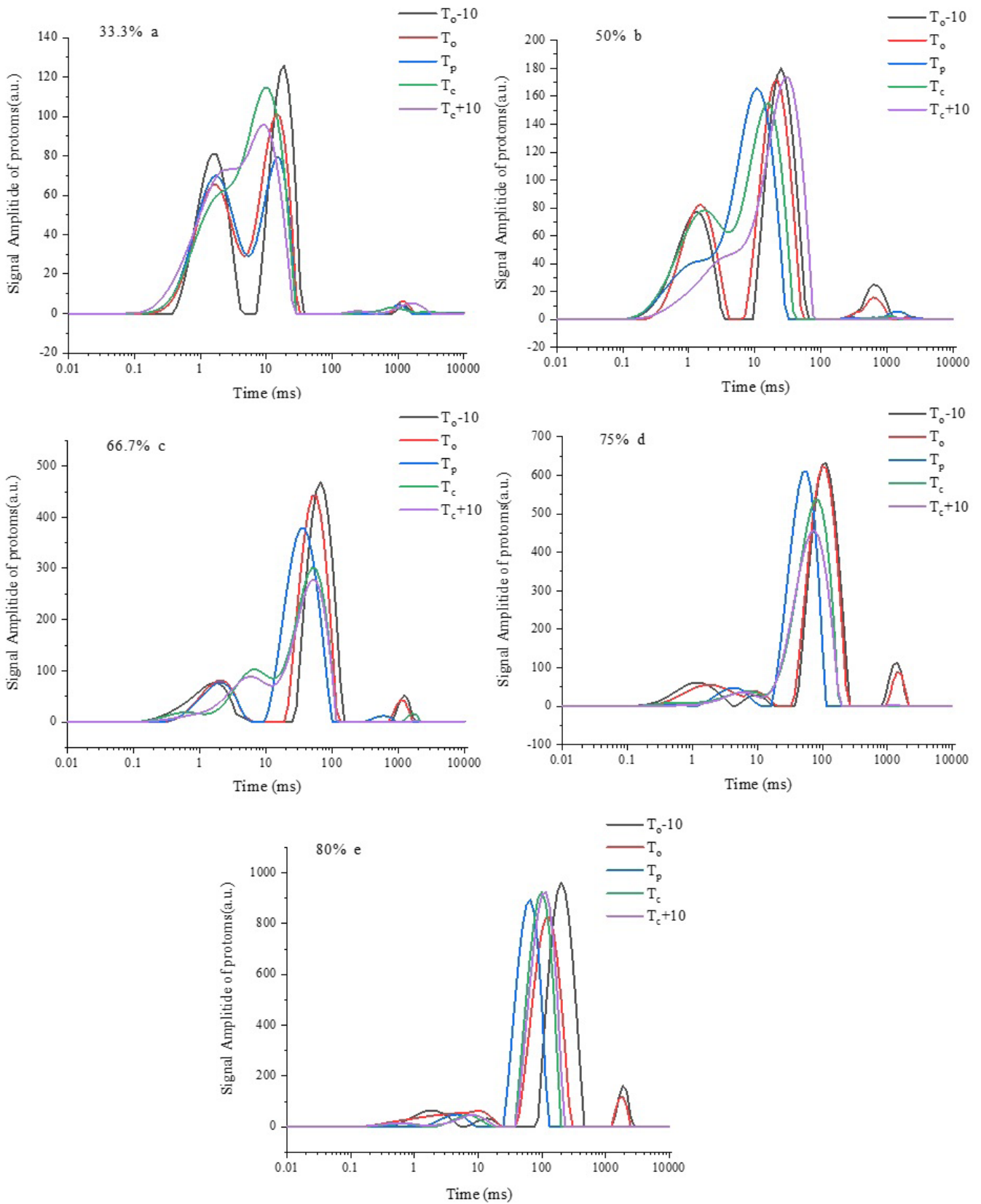


Figure 7. T₂ relaxation diagrams of wheat starch gels with different moisture content.

Table 6. Changes in the total moisture peak area of wheat starch gels with different moisture content.

	A ₂ (%)			
	A ₂₁	A ₂₂	A ₂₃	A ₂₄
33.3%				
T _o -10	46.73 ± 0.0a	55.52 ± 1.3a	-	0.75 ± 0.1b
T _o	47.37 ± 1.2a	51.15 ± 1.2b	-	1.14 ± 0.3a
T _p	58.33 ± 1.2b	40.45 ± 1.0c	-	1.09 ± 0.0a
T _c	98.68 ± 0.0c	-	0.58 ± 1.3a	0.72 ± 0.1b
T _c +10	98.63 ± 0.0c	-	0.85 ± 1.0b	0.47 ± 0.1c
50%				
T _o -10	34.19 ± 1.5b	59.35 ± 2.1a	6.15 ± 1.4a	1.40 ± 0.0a
T _o	35.23 ± 2.1b	60.54 ± 1.3a	3.98 ± 1.0b	0.93 ± 0.0a
T _p	98.60 ± 1.5a	-	8.83 ± 0.4c	0.76 ± 0.0c
T _c	99.03 ± 0.0a	-	15.37 ± 1.3d	0.31 ± 0.0b
T _c +10	99.16 ± 0.0a	-	18.49 ± 0.5e	0.26 ± 0.1b
66.7%				
T _o -10	20.42 ± 1.0b	75.82 ± 2.3b	-	3.76 ± 0.3a
T _o	19.10 ± 1.7c	77.43 ± 1.6c	-	3.47 ± 0.0a
T _p	16.55 ± 1.5d	82.68 ± 1.2d	-	0.77 ± 0.1b
T _c	30.75 ± 2.0a	68.15 ± 1.5a	-	1.09 ± 0.1c
T _c +10	30.83 ± 1.0a	69.07 ± 1.2a	-	
75%				
T _o -10	11.77 ± 1.3b	2.57 ± 0.1b	78.91 ± 1.0a	6.47 ± 0.2b
T _o	12.57 ± 1.0c	3.32 ± 0.0a	79.43 ± 2.0a	4.69 ± 1.2c
T _p	1.03 ± 0.1c	9.79 ± 2.1c	88.94 ± 0.0b	
T _c	3.50 ± 1.2a	7.67 ± 1.3d	88.45 ± 0.0b	
T _c +10	3.72 ± 0.0a	3.27 ± 1.1a	88.77 ± 1.3b	
80%				
T _o -10	7.93 ± 0.4a	2.15 ± 1.5b	84.05 ± 0.0b	5.87 ± 1.2a
T _o	1.44 ± 0.1b	15.01 ± 2.0c	80.59 ± 1.6c	4.40 ± 1.6b
T _p	0.33 ± 0.0c	5.59 ± 1.3a	94.09 ± 1.7a	-
T _c	1.67 ± 0.2b	5.14 ± 1.5a	93.15 ± 2.1a	-
T _c +10	2.06 ± 0.3d	5.57 ± 1.0a	92.37 ± 1.3a	-

Note: The values are mean ± standard deviation, different letters in the same column indicated significant difference (P < 0.05).

peak area of bound water increases gradually. At this time, the peak area of free water and non-flowable water changes little; When the moisture content was 66.7%, the free water gradually decreased to 0, the bound water gradually increased, and the uneasy flowing water first increased and then decreased. It may be the case that when the temperature was low, free water was mainly converted to nonflowable water, and when the temperature was high, free water was mainly converted to bound water; When the water content was 75% and 80%, and samples were heated to T_p, T_c, T_c+10, the free water content was 0. The combined water peak area decreases first and then increases, and the uneasy water peak area increases first and then decreases.

4 Conclusion

The phase transition of Bainong 365 wheat starch under different moisture content was studied by preheating samples in a RVA to simulate DSC heating profiles. When heating to the end temperature of the endothermic transformation or beyond, the enthalpy was 0, all free water was converted into uneasy flowing water and bound water, the granular structure

on the starch surface was severely damaged, and DSC, NMR and SEM results showed that starch gelled completely. However the R_{1047/1022} ratio and relative crystallinity were not 0, including that the short-range and long-range structure of starch was not completely destroyed, FTIR and XRD results showed that the starch did not gel completely. We believe that the endothermic transition temperature range of starch does not represent the complete gelation temperature range of starch, Moreover, the structure destroyed by starch gelation may not simply refer to the short-range and long-range ordered structure of starch

Availability of data and material

All data used during the study are available in a repository or online in accordance with funder data retention policies (Provide full citations that include URLs or DOIs.)

Funding

Supported the National Natural Science Foundation, China, Project No. 32072180.

Scientific and Technological Project in Henan Province, China, Project No. 212102110349.

Key Science and Technology projects of Henan Province, China, Project No. 151100110700.

References

- An, D., Li, Q., Li, E., Obadi, M., Li, C., Li, H., Zhang, J., Du, J., Zhou, X., Li, N., & Xu, B. (2021). Structural basis of wheat starch determines the adhesiveness of cooked noodles by affecting the fine structure of leached starch. *Food Chemistry*, 341(Part 1), 128222. <http://dx.doi.org/10.1016/j.foodchem.2020.128222>. PMID:33065469.
- Chen, B., Zeng, S., Zeng, H., Guo, Z., Zhang, Y., & Zheng, B. (2017). Slowly digestible properties of lotus seed starch-glycerine monostearin complexes formed by high pressure homogenization. *Food Chemistry*, 226, 119-127. <http://dx.doi.org/10.1016/j.foodchem.2017.01.018>. PMID:28254001.
- Chen, P., Liu, X., Zhang, X., Sangwan, P., & Yu, L. (2015). Phase Transition of Waxy and Normal Wheat Starch Granules during Gelatinization. *International Journal of Polymer Science*, 2015, 1-7. <http://dx.doi.org/10.1155/2015/397128>.
- Chen, P., Yu, L., Simon, G. P., Liu, X., Dean, K., & Chen, L. (2011). Internal structures and phase-transitions of starch granules during gelatinization. *Carbohydrate Polymers*, 83(4), 1975-1983. <http://dx.doi.org/10.1016/j.carbpol.2010.11.001>.
- Chrastil, J. (1987). Improved colorimetric determination of amylose in starches of flours. *Carbohydrate Research*, 159(1), 154-158. [http://dx.doi.org/10.1016/S0008-6215\(00\)90013-2](http://dx.doi.org/10.1016/S0008-6215(00)90013-2).
- Colussi, R., Kringel, D., Kaur, L., Zavareze, E. R., & Singh, J. (2020). Dual modification of potato starch: effects of heat-moisture and high pressure treatments on starch structure and functionalities. *Food Chemistry*, 318, 126475. <http://dx.doi.org/10.1016/j.foodchem.2020.126475>. PMID:32135422.
- Donovan, J. W. (1979). Phase transitions of the starch-water system. *Biopolymers: Original Research on Biomolecules*, 18(2), 263-275. <http://dx.doi.org/10.1002/bip.1979.360180204>.
- EE, K. Y., Eng, M. K., & Lee, M. L. (2020). Physicochemical, thermal and rheological properties of commercial wheat flours and corresponding starches. *Food Science and Technology*, 40(Suppl 1.), 51-59. <http://dx.doi.org/10.1590/fst.39718>.
- Fan, D., Ma, S., Wang, L., Zhao, H., Zhao, J., Zhang, H., & Chen, W. (2013). ¹H NMR studies of starch-water interactions during microwave heating. *Carbohydrate Polymers*, 97(2), 406-412. <http://dx.doi.org/10.1016/j.carbpol.2013.05.021>. PMID:23911464.
- Gerçekaslan, K. E. (2021). Hydration level significantly impacts the freezeable- and unfreezeable-water contents of native and modified starches. *Food Science and Technology*, 41(2), 426-431. <http://dx.doi.org/10.1590/fst.04520>.
- Gilbert, R. G., Witt, T., & Hasjim, J. (2013). What is being learned about starch properties from multiple-level characterization. *Cereal Chemistry*, 90(4), 312-325. <http://dx.doi.org/10.1094/CCHEM-11-12-0141-FI>.
- Hansen, M. R., Blennow, A., Farhat, I., Norgaard, L., Pedersen, S., & Engelsen, S. B. (2009). Comparative NMR relaxometry of gels of amyloamylase-modified starch and gelatin. *Food Hydrocolloids*, 23(8), 2038-2048. <http://dx.doi.org/10.1016/j.foodhyd.2009.05.008>.
- Hung, P. V., Maeda, T., & Morita, N. (2007). Study on physicochemical characteristics of waxy and high-amylose wheat starches in comparison with normal wheat starch. *Starch*, 59(3-4), 125-131. <http://dx.doi.org/10.1002/star.200600577>.
- Jiang, J., Gao, H., Zeng, J., Zhang, L., Wang, F., Su, T., & Li, G. (2021). Determination of subfreezing temperature and gel retrogradation characteristics of potato starch gel. *Lebensmittel-Wissenschaft + Technologie*, 149, 112037. <http://dx.doi.org/10.1016/j.lwt.2021.112037>.
- Kovrljica, R., & Rondeau-Mouro, C. (2017). Hydrothermal changes of starch monitored by combined nmr and dsc methods. *Food and Bioprocess Technology*, 10(3), 445-461. <http://dx.doi.org/10.1007/s11947-016-1832-9>.
- Li, Y., Shi, W., Cheng, S., Wang, H., & Tan, M. (2017). Freezing-induced proton dynamics in tofu evaluated by low-field nuclear magnetic resonance. *Journal of Food Measurement and Characterization*, 11(3), 1003-1010. <http://dx.doi.org/10.1007/s11694-017-9475-8>.
- Oliveira, D. I., Demogalski, L., Dias, A. H., Pereira, L. A. A., Alberti, A., Los, P. R., & Demiate, I. M. (2021). Traditional sour cassava starch obtained with alterations in the solar drying stage. *Food Science and Technology*, 41(Suppl. 1), 319-327. <http://dx.doi.org/10.1590/fst.16120>.
- Ozel, B., Dag, D., Kilercioglu, M., Sumnu, S. G., & Oztop, M. H. (2017). NMR relaxometry as a tool to understand the effect of microwave heating on starch-water interactions and gelatinization behavior. *Lebensmittel-Wissenschaft + Technologie*, 83, 10-17. <http://dx.doi.org/10.1016/j.lwt.2017.04.077>.
- Ratnayake, W. S., & Jackson, D. S. (2007). A new insight into the gelatinization process of native starches. *Carbohydrate Polymers*, 67(4), 511-529. <http://dx.doi.org/10.1016/j.carbpol.2006.06.025>.
- Schirmer, M., Jekle, M., & Becker, T. (2015). Starch gelatinization and its complexity for analysis. *Starch*, 67(1-2), 30-41. <http://dx.doi.org/10.1002/star.201400071>.
- Selma-Gracia, R., Laparra, J. M., & Haros, C. M. (2020). Potential beneficial effect of hydrothermal treatment of starches from various sources on in vitro digestion. *Food Hydrocolloids*, 103, 105687. <http://dx.doi.org/10.1016/j.foodhyd.2020.105687>.
- Shang, L., Wu, C., Wang, S., Wei, X., Li, J., & Li, J. (2021). The influence of amylose and amylopectin on water retention capacity and texture properties of frozen-thawed konjac glucomannan gel. *Food Hydrocolloids*, 113, 106521. <http://dx.doi.org/10.1016/j.foodhyd.2020.106521>.
- Su, C., Saleh, A. S. M., Zhang, B., Zhao, K., Ge, X., Zhang, Q., & Li, W. (2020). Changes in structural, physicochemical, and digestive properties of normal and waxy wheat starch during repeated and continuous annealing. *Carbohydrate Polymers*, 247, 116675. <http://dx.doi.org/10.1016/j.carbpol.2020.116675>. PMID:32829803.
- Sun, S., Jin, Y., Hong, Y., Gu, Z., Cheng, L., Li, Z., & Li, C. (2021). Effects of fatty acids with various chain lengths and degrees of unsaturation on the structure, physicochemical properties and digestibility of maize starch-fatty acid complexes. *Food Hydrocolloids*, 110, 106224. <http://dx.doi.org/10.1016/j.foodhyd.2020.106224>.
- Van Soest, J., Tournois, H., de Wit, D. D., & Vliegthart, J. (1995). Short-range structure in (partially) crystalline potato starch determined with attenuated total reflectance Fourier-transform IR spectroscopy. *Carbohydrate Research*, 279, 201-214. [http://dx.doi.org/10.1016/0008-6215\(95\)00270-7](http://dx.doi.org/10.1016/0008-6215(95)00270-7).
- Vermeulen, R., Goderis, B., Reynaers, H., & Delcour, J. A. (2005). Gelatinisation related structural aspects of small and large wheat starch granules. *Carbohydrate Polymers*, 62(2), 170-181. <http://dx.doi.org/10.1016/j.carbpol.2005.07.021>.
- Waigh, T. A., Gidley, M. J., Komanshek, B. U., & Donald, A. M. (2000). The phase transformations in starch during gelatinisation: a liquid crystalline approach. *Carbohydrate Research*, 328(2), 165-176. [http://dx.doi.org/10.1016/S0008-6215\(00\)00098-7](http://dx.doi.org/10.1016/S0008-6215(00)00098-7). PMID:11028784.

- Wang, S., & Copeland, L. (2013). Molecular disassembly of starch granules during gelatinization and its effect on starch digestibility: a review. *Food & Function*, 4(11), 1564-1580. <http://dx.doi.org/10.1039/c3fo60258c>. PMID:24096569.
- Wang, S., Wang, J., Zhang, W., Li, C., Yu, J., & Wang, S. (2015). Molecular order and functional properties of starches from three waxy wheat varieties grown in China. *Food Chemistry*, 181, 43-50. <http://dx.doi.org/10.1016/j.foodchem.2015.02.065>. PMID:25794719.
- Wang, S., Wang, S., Liu, L., Wang, S., & Copeland, L. (2017). Structural orders of wheat starch do not determine the in vitro enzymatic digestibility. *Journal of Agricultural and Food Chemistry*, 65(8), 1697-1706. <http://dx.doi.org/10.1021/acs.jafc.6b04044>. PMID:28161950.
- Wang, S., Zhang, X., Wang, S., & Copeland, L. (2016). Changes of multi-scale structure during mimicked DSC heating reveal the nature of starch gelatinization. *Scientific Reports*, 6(1), 28271. <http://dx.doi.org/10.1038/srep28271>. PMID:27319782.
- Xu, J., Blennow, A., Li, X., Chen, L., & Liu, X. (2020). Gelatinization dynamics of starch in dependence of its lamellar structure, crystalline polymorphs and amylose content. *Carbohydrate Polymers*, 229, 115481. <http://dx.doi.org/10.1016/j.carbpol.2019.115481>. PMID:31826407.
- Yao, Y., & Ding, X. (2002). Pulsed Nuclear Magnetic Resonance (PNMR) study of rice starch retrogradation. *Cereal Chemistry*, 79(6), 751-756. <http://dx.doi.org/10.1094/CCHEM.2002.79.6.751>.
- Zhang, H., Zhang, W., Xu, C., & Zhou, X. (2013). Morphological features and physicochemical properties of waxy wheat starch. *International Journal of Biological Macromolecules*, 62, 304-309. <http://dx.doi.org/10.1016/j.ijbiomac.2013.09.030>. PMID:24076202.
- Zhang, L., Zeng, L., Wang, X., He, J., & Wang, Q. (2020). The influence of Konjac glucomannan on the functional and structural properties of wheat starch. *Food Science & Nutrition*, 8(6), 2959-2967. <http://dx.doi.org/10.1002/fsn3.1598>. PMID:32566214.
- Zhang, Y., Chen, C., Chen, Y., & Chen, Y. (2019). Effect of rice protein on the water mobility, water migration and microstructure of rice starch during retrogradation. *Food Hydrocolloids*, 91, 136-142. <http://dx.doi.org/10.1016/j.foodhyd.2019.01.015>.
- Zhao, T., Li, X., Ma, Z., Hu, X., Wang, X., & Zhang, D. (2020). Multiscale structural changes and retrogradation effects of addition of sodium alginate to fermented and native wheat starch. *International Journal of Biological Macromolecules*, 163, 2286-2294. <http://dx.doi.org/10.1016/j.ijbiomac.2020.09.094>. PMID:32961185.